Effect of convection on the summertime extratropical lower stratosphere

A. E. Dessler
Earth Systems Science Interdisciplinary Center, University of Maryland, College Park, Maryland, USA

S. C. Sherwood
Department of Geology and Geophysics, Yale University, New Haven, Connecticut, USA

Received 7 July 2004; revised 31 August 2004; accepted 21 September 2004; published 2 December 2004.

[1] Satellite and in situ water vapor and ozone observations near the base of the overworld ($\theta \approx$ 380-K potential temperature) are examined in summertime northern midlatitudes, with a focus on how their horizontal variations are influenced by deep convection. We show that summertime convection has a significant effect on the water vapor budget here, but only a small effect on the ozone budget. Using a simple model, we estimate that convection increases model extratropical water vapor at 380 K by 40% but decreases model extratropical ozone by only a few percent, relative to what would occur without convection. In situ data show that this convective injection occurs up to at least ~390 K. This raises the possibility that the convectively moistened air might travel isentropically to the tropics and ascend into the stratospheric overworld without passing through the cold point. We argue that trends in convective moistening should be examined as possible contributors to observed trends in lower stratospheric water vapor, at least during summer months. *INDEX TERMS:* 0368 Atmospheric Composition and Structure: Troposphere—constituent transport and chemistry; 0322 Atmospheric Composition and Structure: Constituent sources and sinks; 0320 Atmospheric Composition and Structure: Cloud physics and chemistry; *KEYWORDS:* extratropical convection, extratropical tropopause, stratosphere-troposphere exchange, lower stratospheric ozone, lower stratospheric water vapor

Citation: Dessler, A. E., and S. C. Sherwood (2004), Effect of convection on the summertime extratropical lower stratosphere, *J. Geophys. Res.*, *109*, D23301, doi:10.1029/2004JD005209.

1. Introduction

[2] The mechanisms that determine the chemical composition of the upper troposphere/lower stratosphere (UT/LS) are of considerable interest to the scientific community. One process in particular, vertical transport via deep convection, has been the subject of much recent debate. In the tropics, convection to the altitude of the tropopause and above does occur [e.g., *Alcala and Dessler*, 2002; *Gettelman et al.*, 2002] and appears to play a role in determining the abundance of trace species there [e.g., *Dessler*, 2002]. In the extratropics the canonical view has been that the lowermost stratosphere, bounded at the bottom by the extratropical tropopause and the top by the 380-K potential temperature (θ) surface, is primarily influenced by horizontal, isentropic transport from the tropical upper troposphere and by slow downwelling from the stratosphere above, but not to a great extent by extratropical deep convection [e.g., *Holton et al.*, 1995].

[3] There is, however, plenty of anecdotal evidence that extratropical convection does penetrate well into the lowermost stratosphere [e.g., *Roach*, 1967; *Poulida et al.*, 1996; *Fischer et al.*, 2003], and even into the overworld ($\theta >$ 380 K) [*Fromm and Servranckx*, 2003; *Fromm et al.*, 2000; *Wang*, 2003; *Jost et al.*, 2004; *Livesey et al.*, 2004] (see, e.g., *Hoskins* [1991] or *Holton et al.* [1995] for definitions and a discussion of the overworld and lowermost stratosphere). A key question is whether these penetrations are simple curiosities, or important in the constituent budget of the lowermost stratosphere or overworld.

[4] To illustrate the problem, we plot in Figure 1 the vertical distribution of water vapor (H_2O) volume mixing ratio (VMR) measured by instruments on NASA's WB-57 aircraft during the Cirrus Regional Study of Tropical Anvils and Cirrus Layers–Florida Area Cirrus Experiment (CRYSTAL-FACE). Only those measurements with coincident measurements of O_3 VMR > 400 ppbv are shown here. The data were obtained on flights out of Key West Naval Air Station, Florida, United States (24°N, 82°W), during July 2002, at latitudes between 14°N and 27°N.

[5] Figure 1 shows that for $\theta >$ ~400 K, H_2O VMRs are 4.5–6.0 ppmv. These are quite typical values for the overworld, and are explained by dehydration to around 3.85 ppmv at the tropical tropopause [e.g., *Dessler and Kim*, 1999] combined with production of H_2O from CH_4 and H_2 oxidation [e.g., *Wofsy et al.*, 1972; *Ehhalt and Tönnißen*, 1979]. At and below ~390 K, H_2O VMRs well

0148-0227/04/2004JD005209$09.00

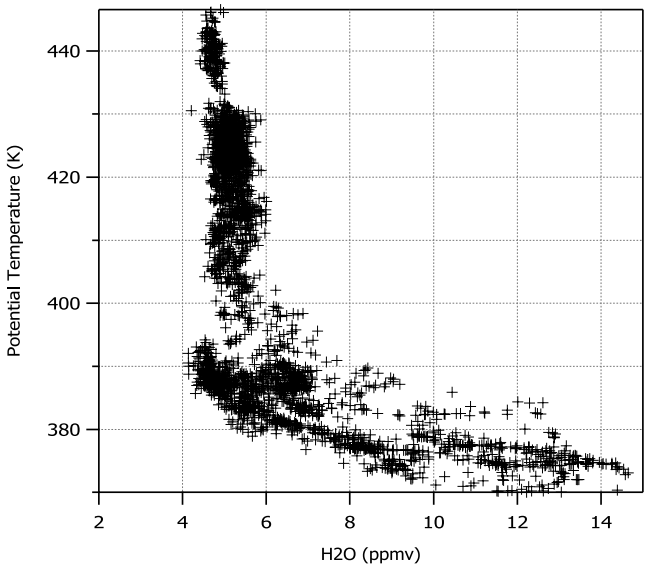

Figure 1. Water vapor VMR (ppmv) versus potential temperature (K) measured during the CRYSTAL-FACE mission in July 2002. Only points with corresponding O_3 VMRs greater than 400 ppbv are shown. The water vapor instrument is described by *Weinstock et al.* [1994]; the O_3 instrument is described by *Proffitt and McLaughlin* [1983]; temperature and pressure measurements were made by the NOAA pressure/temperature instrument suite.

above these stratospheric values are evident. Since these high values could not have descended from the overworld, some of this air must have come from the troposphere, either by local moist convection or quasi-horizontal eddy transport from the tropical upper troposphere. On the other hand, the O_3 values associated with these measurements (>400 ppbv) are several times greater than typical tropospheric values and are therefore inconsistent with a tropospheric source, suggesting instead an overworld origin for the air. This presents a dilemma. We will show that this dilemma can be resolved by properly accounting for both convective mixing and large-scale transport.

[6] We will focus in this paper on the region around the 380-K θ surface. This surface is near the tropopause in the tropics, but well within the stratosphere in the extratropics. In the extratropics, the 380-K surface serves as the boundary between the overworld ($\theta > 380$) and the lowermost stratosphere (stratospheric air with $\theta < 380$). This is a significant demarcation. Air injected into the lowermost stratosphere will remain in the stratosphere for at most a few months, while air injected into the extratropical overworld has the possibility of experiencing relatively rapid isentropic transport to lower latitudes [*Minschwaner et al.*, 1996], where it can be lofted throughout the stratosphere, resulting in a much longer residence time. Since 380 K is just above the typical location of the tropical cold point (~375 K), air following this path can in principle enter the overworld without passing through the tropical cold point. Finally, if the influence of convection does extend to 380 K, it strongly suggests that convection will influence all altitudes below this.

[7] Satellite data can provide a much broader view of the H_2O and O_3 distributions. Figure 2 shows the distribution of

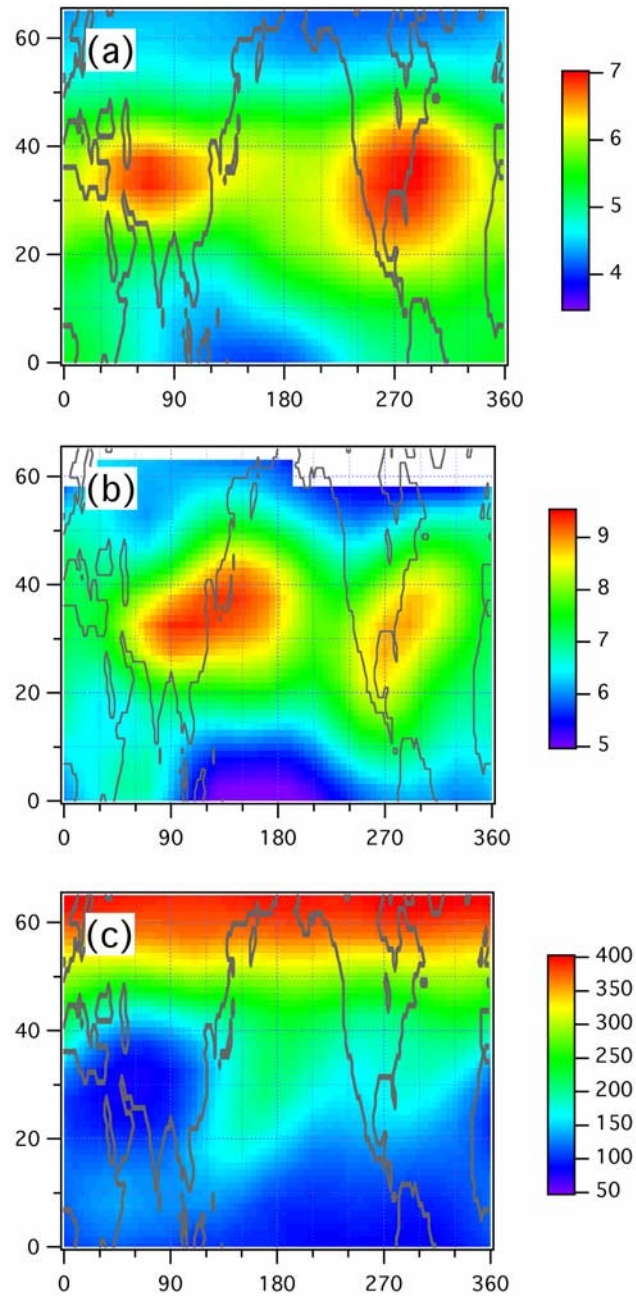

Figure 2. (a and b) Average H_2O VMR (ppmv) and (c) average O_3 VMR (ppbv) at 380-K θ. Data in Figures 2a and 2c were measured by HALOE between 15 June and 15 August of 1993 through 1999; data in Figure 2b were measured by the MLS during 16 days in July 1992. The θ of each measurement is determined using daily temperature and pressure fields from the United Kingdom Meteorological Office (UKMO) [*Swinbank and O'Neill*, 1994], and linear interpolation is used to determine the VMR at 380 K. The MLS and HALOE H_2O data have been adjusted, as described in the data section. For the MLS data, only measurements at 147 hPa and higher altitudes have been used.

H_2O and O_3 for July on the 380-K surface from two instruments on the Upper Atmosphere Research Satellite (UARS) [e.g., *Dessler et al.*, 1998]: the Halogen Occultation Experiment (HALOE) [*Russell et al.*, 1993] and the Microwave Limb Sounder (MLS) [*Barath et al.*, 1993]. The HALOE data are version 19 and cover the period from 1993 to 1999. In response to a recognized low bias in the HALOE H_2O measurements [*Stratospheric Processes and their Role in Climate* (*SPARC*), 2000, section 2.3.1], we have multiplied the V19 VMRs by factors of 1.20, 1.10, and 1.05 for pressure levels of 121 hPa, 100–68 hPa, and 56 hPa, respectively (E. E. Remsberg, personal communication, 2004). The MLS data have been processed using a new H_2O algorithm, known as version 7.02 [*Read et al.*, 2004] and cover 16 days in July 1992. As suggested by Read et al., we have increased MLS H_2O at 147 hPa by 30% and at 100 hPa by 20%.

[8] There is broad agreement between the HALOE and MLS H_2O data in Figures 2a and 2b. Both show maxima over the Asian monsoon (70°E, 35°N) and over North America (270°E, 30°N), although the shapes of the maxima are different. It seems reasonable that these maxima are likely the result of intense continental convection over these two regions, as suggested by *Randel et al.* [2001]. Despite the adjustments described in the last paragraph, an offset between the instruments remains, with the MLS measuring several ppmv higher than the HALOE at this altitude. Some of the differences, such as the shapes of the maxima, are probably due to the different time periods covered and the length of the two data sets. Other differences, such as the offset, likely represent real differences in the measurements, and must be considered a measure of the uncertainty of our knowledge of H_2O at 380 K. See *Read et al.* [2004] for a more detailed intercomparison between the data sets.

[9] Figure 2c shows the O_3 distribution measured by the HALOE. Coincident with the H_2O maximum over the Asian monsoon is an O_3 minimum. One might view this as consistent: the convective detrainment that contains high H_2O VMRs also contains low O_3 VMRs, so this association between high H_2O and low O_3 makes sense. This interpretation, however, runs into problems over North America. Here, both data sets again show an H_2O maximum. However, there is no associated low-O_3 region. This is a different view of the same conundrum posed by the in situ data in Figure 1: air with high H_2O VMRs, consistent with convection, but also high O_3 VMRs, inconsistent with convection. Another puzzle is that the values of H_2O VMR found in the H_2O maximum over North America are comparable to those found over the Asian monsoon maximum. This should be surprising since the Asian monsoon is a region of far more vigorous convection than North America [e.g., *Dunkerton*, 1995].

[10] In this paper, we will quantitatively explain how convection affects H_2O and O_3. In particular, we will show that convection can affect different tracers differently, so that the O_3 field is not affected in the same way as the H_2O field. In this way, we will explain the different O_3-H_2O relations over Asia and North America.

2. Convective Contrast

[11] To begin to explain the satellite and in situ data, we cast the convective tendency for trace gas X at a point in space as a relaxation toward a target concentration $[X]_c$ with a time constant τ_c:

$$\frac{\partial [X]}{\partial t} = -\frac{1}{\tau_c}\left([X] - [X]_c\right). \quad (1)$$

The time constant τ_c is the reciprocal of the rate at which air is convectively exchanged between the detrainment level and the source region, and we expect it to be the same for all constituents. The target concentration $[X]_c$ is the convective equilibrium abundance that would be approached if all other processes ceased; for O_3 and most other trace gases, it is closely related to the abundance of constituent X in the planetary boundary layer (PBL).

[12] H_2O, however, can condense and sediment out on timescales much less than τ_c. As a result, the target concentration $[H2O]_c$ is not related to the abundance in the PBL, but instead is related to the local thermodynamic properties of the UT/LS. The idea is that strong updrafts associated with deep convection can carry significant amounts of ice to the UT/LS [e.g., *Alcala and Dessler*, 2002]. Evaporation of ice deposited into the UT/LS will tend to drive the region toward saturation, with excess ice sedimenting out. In other words, convection drives the local atmosphere toward saturation, so $[H_2O]_c$ is equal to the local saturation VMR, $[H_2O]^*$. We plot zonally averaged $[H_2O]^*$ as a function of latitude in Figure 3a. Note that the saturation VMR increases rapidly with latitude, from a few ppmv between 10°N and 10°S, to hundreds of ppmv poleward of 40°N.

[13] We will refer to $[X]$-$[X]_c$ as the "convective contrast" for species X. As the convective contrast increases, equation (1) suggests that the effect of convection on the abundance of constituent X also increases. At most latitudes at 380 K, $[H_2O]_c \gg [H_2O]$, so Figure 3a is to a good approximation equal to the convective contrast for H_2O. The increasing convective contrast with latitude means that a single convective event, everything else being equal, will transport more H_2O to the 380-K surface as the location of the convective event moves poleward.

[14] The convective contrast for O_3, $[O_3]$-$[O_3]_c$, also increases with latitude as the background 380-K O_3 VMR increases, but much more slowly. To see the implications of this, we plot in Figure 3b the absolute value of the ratio of the fractional changes in H_2O to the fractional change in O_3 per unit time:

$$\left| \left(\frac{-\frac{1}{\tau_c}\left([H_2O] - [H_2O]_c\right)}{[H_2O]} \right) \Big/ \left(\frac{-\frac{1}{\tau_c}\left([O_3] - [O_3]_c\right)}{[O_3]} \right) \right| \quad (2)$$

(note that the convective time constant τ appears in both the numerator and denominator and therefore cancels out). Near the equator, this ratio is near one, meaning that there is a similar fractional change in H_2O and O_3 per unit convection. As one heads poleward, however, this ratio rapidly rises, indicating that the fractional change in H_2O per convective event becomes much larger relative to the fractional change in O_3. This is a direct result of the rapid increase in convective contrast of H_2O shown in Figure 3a. In other words, convection occurring at high latitudes is

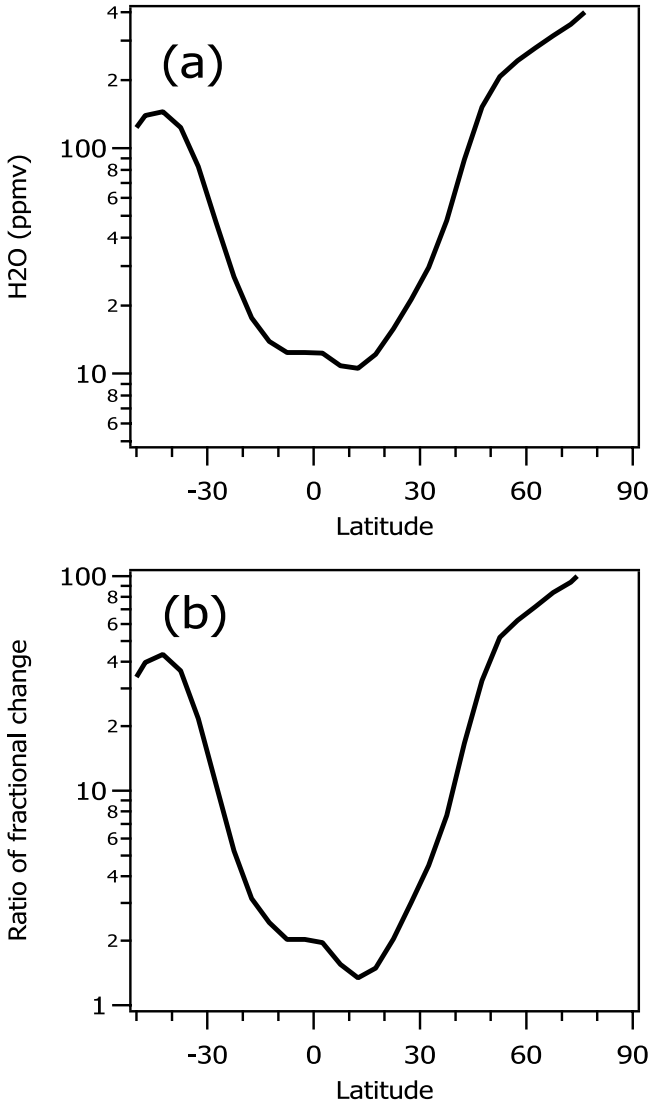

Figure 3. (a) Plot of zonally averaged H_2O saturation VMR at 380 K as a function of latitude, based on UKMO temperature fields for July 1992. Because the saturation VMR $\gg$ the ambient H_2O VMR at most latitudes, this plot is to a good approximation also the convective contrast. (b) Ratio of fractional change in $[H_2O]$ to $[O_3]$ per unit of convection (equation (2)). Calculated using the zonally averaged HALOE H_2O and O_3 fields from Figure 2 and the H_2O saturation VMR from Figure 3a as $[H_2O]_c$. $[O_3]_c$ is assumed to be zero, which assumes a maximum convective effect on O_3.

expected to perturb the H_2O abundance to a much greater degree than the O_3 abundance.

3. Single-Level Isentropic Model

[15] To investigate the issues discussed above more quantitatively, we have developed a single-level isentropic model, which simulates H_2O and O_3 on the 380-K θ surface. The model is driven by UKMO horizontal winds [*Swinbank and O'Neill*, 1994], interpolated to the 380-K level. The horizontal advection is carried out by a semi-Lagrangian advection scheme [*Stainforth and Cote*, 1991] with a time step of 15 min.

[16] Vertical transport must be parameterized in this model. Once per day, we apply a tendency to account for the Brewer-Dobson circulation, which is a large-scale, slow upwelling at low latitudes and downwelling at high latitudes. The tendency term due to this circulation is parameterized as a relaxation:

$$\left.\frac{\partial[\mathrm{X}]}{\partial t}\right|_{\mathrm{BD}} = \frac{1}{\tau_{\mathrm{BD}}}\left([\mathrm{X}] - [\mathrm{X}]_{\mathrm{BD}}\right), \tag{3}$$

where X is H_2O or O_3. $[O_3]_{BD}$, is assumed to be 75 ppbv for regions of upward motion, and 425 ppbv for regions of downward motion. $[H_2O]_{BD}$ is 10 ppmv and 4 ppmv for upward and downward motion, respectively. The values of these parameters are set within a range constrained by our knowledge of the TTL, but within that range are adjusted to produce optimal agreement between the model and the satellite measurements. We will discuss the sensitivity of the model to these parameters and its effect on our overall results later in the paper.

[17] The Brewer-Dobson circulation time constant τ_{BD} is a function of latitude and longitude and is equal to $C_1/|\partial\theta/\partial t|$, where $|\partial\theta/\partial t|$ is the absolute value of the local 380-K daily heating rate (heating rates are calculated according to *Rosenfield et al.* [1994]). The constant C_1 is chosen to give a time constant of $\sim$60 days in the tropics. This leads to Brewer-Dobson relaxation timescales of 20–30 days at high latitudes.

[18] Also once per day, we apply a tendency to account for convection in regions where deep convection is occurring. We parameterize the convective tendency according to equation (1), with $[O_3]_c$ of 75 ppbv and $[H_2O]_c$ equal to the local saturation VMR. For estimates of τ_c, we use observations of outgoing longwave radiance from satellites to indicate the location of deep convection.

[19] Figure 4 plots the fraction of pixels with 11-μm brightness temperatures less than 210 K, f_{conv}, during July

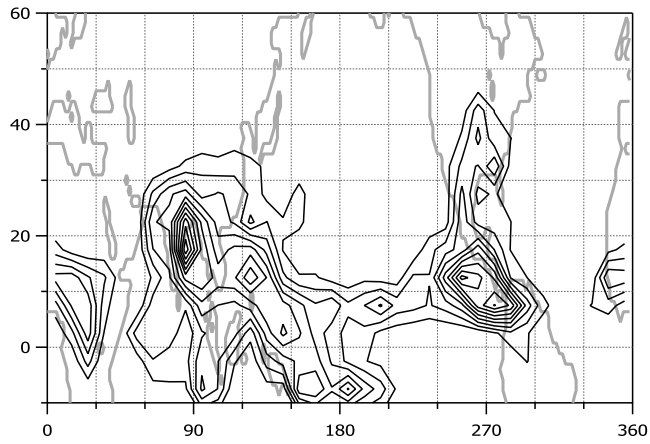

Figure 4. Fraction of 11-μm radiance observations with brightness temperature < 210 K during July 1992. The outer contour is 1%, with contours progressively increasing by 1%. Data from the morning and afternoon overpasses of the NOAA 11 and 12 satellites, as stored in the International Satellite Cloud Climatology Project's (ISCCP) B3 product.

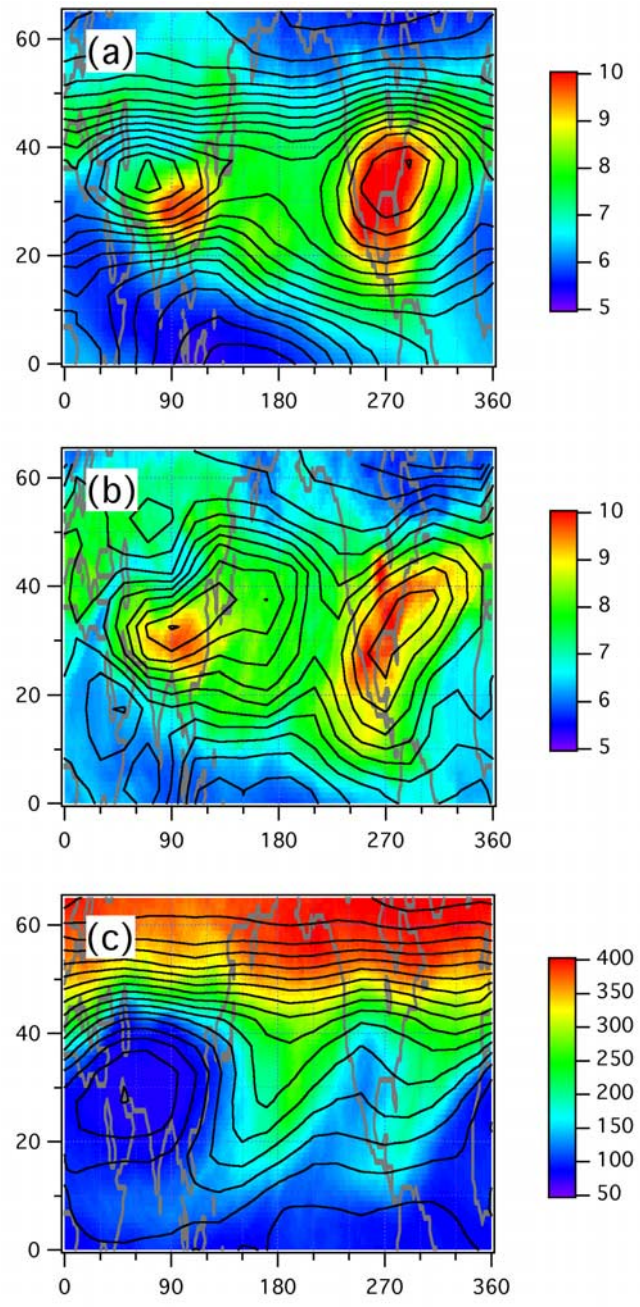

Figure 5. (a and b) Average H_2O VMR (ppmv) and (c) average O_3 VMR (ppbv) at 380-K θ, as simulated by the single-level isentropic model. Data in Figures 5a and 5c are simulations of July 1993–1999; data in Figure 5b are a simulation of July 1992. The contours in each panel are the satellite measurements from the corresponding time period, which was plotted in the corresponding panel of Figure 2.

1992. The data are from the Advanced Very High Resolution Radiometers (AVHRR) on board the NOAA 11 and 12 satellites. The data are from the morning and afternoon overpasses of these satellites, as stored in the International Satellite Cloud Climatology Project's (ISCCP) B3 product. This product contains a small fraction of the original AVHRR data, but at its native 1-km (at nadir) resolution.

[20] One can clearly see the overall distribution of deep convection: frequent in the tropics, with the occurrence dropping off rapidly with latitude. If we assume that $1/\tau_c$ is proportional to f_{conv}, then it becomes clear that convective moistening should be strongly peaked in the midlatitudes: it is the product of two functions, one that increases rapidly with latitude (convective contrast) and the other that decreases rapidly with latitude (convective mass transport).

[21] The convective relaxation time constant τ_c is the same for H_2O and O_3 and is equal to C_2/f_{conv}. The constant C_2 is chosen to give a time constant of 6.5 days at the location of the maximum f_{conv}. This scaling gives an overall convective turnover time for the 380-K surface in the tropics of several weeks, consistent with the results of *Dessler* [2002]. Choosing a constant convective threshold higher than 210 K produces a distribution similar in shape, but with higher frequencies at all locations. By changing the constant C_2 accordingly so that the maximum timescale remains at 6.5 days, similar results are obtained, suggesting our analysis is insensitive to the brightness temperature used to quantify convective transport, given τ_c. We also investigated whether a latitude- and longitude-dependent temperature threshold would be better, since the 380-K surface becomes warmer outside the tropics so a constant threshold may undercount midlatitude convection. For example, we tried a threshold based on the local temperature of the 380-K surface, where we counted a pixel as indicating deep convection if the temperature of the pixel was colder than that. Unfortunately, in midlatitudes the temperature tends toward isothermal well below the 380-K surface, eliminating the possibility of any straightforward relationship between cloud top temperature and height above the tropopause. In the end, we found no single method that was entirely satisfactory, so with a nod toward simplicity we adopt a constant threshold of 210 K.

[22] UKMO temperature and pressure are used to calculate saturation relative humidity (RH). To account for a known warm bias in the UKMO fields [*Randel et al.*, 2000], we adjust the temperatures downward: temperatures below 200 K are reduced by 3 K, temperatures between 200 and 220 K are reduced by an offset that linearly decreases from 3 K at 200 K to 0 at 220 K, temperatures above 220 K are unadjusted.

[23] We used this model to simulate the month of July for each of the years 1992–1999. To establish the initial condition for each July, we first ran the model with initially zonally symmetric O_3 and H_2O distributions using perpetual 1 July winds. When this reached steady state, the resulting O_3 and H_2O fields were then used as the initial condition for a July run using daily winds. Convective relaxation rates were calculated separately for each July using the frequency of occurrence over that month of satellite pixels meeting the 210-K threshold, and did not vary during the month. The July 1992 simulations will be compared with MLS data, while the average of the July 1993–1999 simulations will be compared with the HALOE data.

[24] Figure 5 shows the model results, with the data from Figure 2 plotted as contours. Overall, the simulations of both constituents are good, with the location of maxima and minima well represented. Importantly, the model simulates high H_2O VMRs over both Asia and North America, but low O_3 VMRs only over Asia. The most serious difference

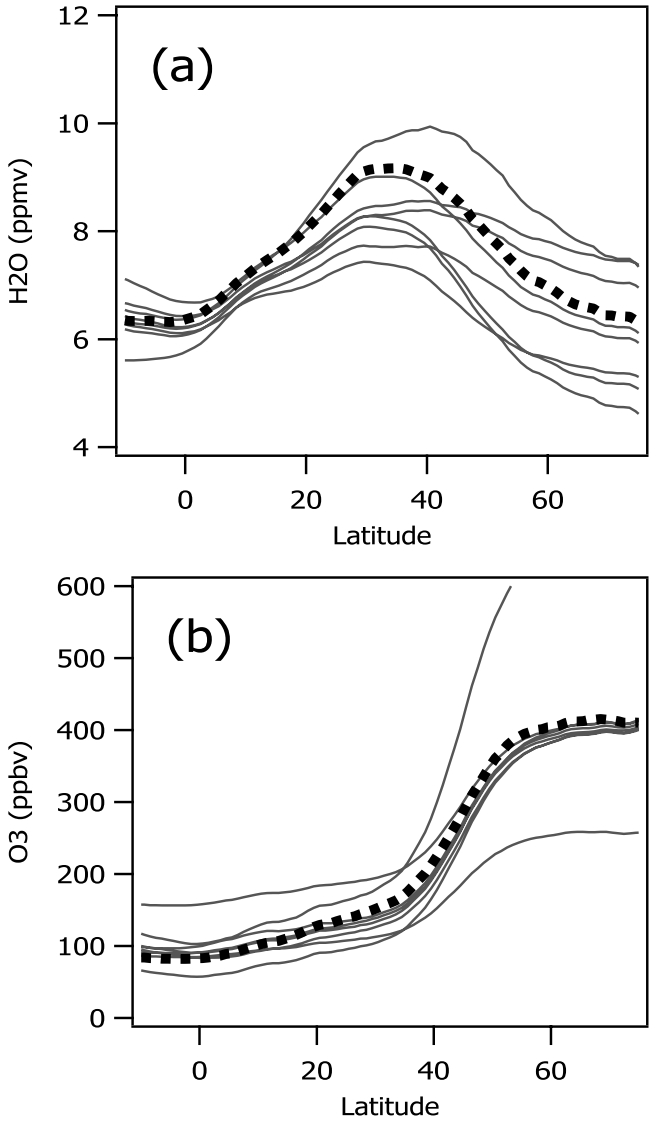

Figure 6. Zonal average of (a) H_2O and (b) O_3 from July 1992 runs of the single-level isentropic model. The thick dotted line is the model run shown in other figures in the paper. The lighter gray lines are runs of the model where we have varied one of the following parameters by a factor of 2: $[O_3]_{BD}$ (values for ascending and descending air are varied independently), τ_{BD}, and τ_c. $[H_2O]_{BD}$ is varied by 2 ppmv. For each of these parameters, we have two runs, one for an increase and one for a decrease.

is in the location of the H_2O maximum associated with the Asian monsoon in the comparison with HALOE data in Figure 5a. The HALOE data show the H_2O maximum located west and poleward of where the model predicts it. It is unclear whether this represents a deficiency in the model or the HALOE data since the MLS data (Figure 5b) show the H_2O maximum close to where the model predicts it. One clue is that in the Asia-West Pacific region the two model calculations are closer to each other, despite the different time periods, than the two observations, suggesting that the latter difference might be instrument-related rather than a result of interannual variability. Clearly, future measurements will be required to sort this out.

[25] To show the sensitivity of the model to the parameters we have chosen, we plot in Figure 6 zonal average H_2O and O_3 abundances from the model calculated after varying the free parameters in the model. At low latitudes, the model-predicted H_2O field is insensitive to the choice of parameters, instead being primarily determined by temperature through the imposed limit of 100% RH. At midlatitudes, the H_2O VMR is sensitive to the choice of the convective turnover time τ_c. This shows that convection is important to the H_2O budget at this altitude unless τ_c is much longer than our best guess value. At high latitudes, both H_2O and O_3 VMRs are most sensitive to the abundance of H_2O and O_3 in air descending as part of the

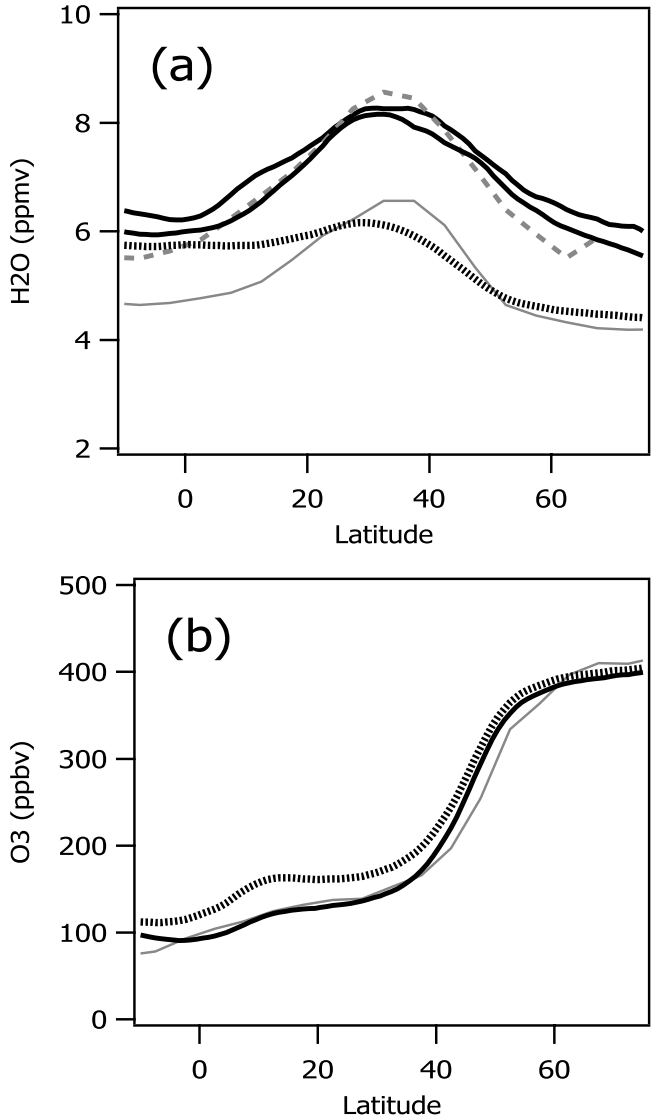

Figure 7. Zonal average of (a) H_2O (ppmv) and (b) O_3 (ppbv) from the HALOE and MLS measurements and the model simulations shown in Figures 2 and 5. The black solid lines are the model simulations from Figure 5 (in the top plot, both the 1992 and 1993–1999 simulations are shown). The black dotted line is the model run (1993–1999) with convection turned off. The gray solid line is the HALOE data, and the gray dashed line is the MLS data, both from Figure 2.

Brewer-Dobson circulation, with high-latitude H_2O also showing some sensitivity to τ_c. In all model runs, however, the midlatitude H_2O peak and the insensitivity of the O_3 fields to convection are robust features. The model is insensitive to the other parameters.

[26] Figure 7 shows zonal averages of modeled and measured H_2O and O_3 at 380 K as a function of latitude. Figure 7a shows that the model agrees well with H_2O measured by the MLS. The model and MLS, however, are both 1–2 ppmv higher than the HALOE data. The CRYSTAL-FACE in situ data in Figure 1, obtained around Florida, show that H_2O at 380 K there ranges between 7 and 13 ppmv, a range that compares well with the model's simulation of ~10 ppmv in that region.

[27] The midlatitude maximum in H_2O VMR is seen in both satellite data sets and its location and magnitude are well reproduced by the model. Also shown on this plot is a model simulation of the HALOE period (1993–1999) where convection has been turned off. This model run shows no midlatitude maximum, suggesting, perhaps unsurprisingly, that convection is responsible.

[28] Figure 7b shows a similar comparison for O_3. The standard model and the HALOE data show good quantitative agreement. The model without convective relaxation shows slightly higher O_3 VMRs at all latitudes, in agreement with our expectations.

[29] To emphasize the effects of convection, Figure 8 plots the differences between the models with and without convection, as a function of latitude. For O_3, the difference is at a maximum at around 10°N, where convective mass flux to the UT/LS is a maximum (see Figure 4). Convection does play a role in regulating the abundance of O_3 here, in agreement with a previous analysis [*Dessler*, 2002]. For H_2O, however, the impact of convection maximizes between 30°N and 50°N, but is important throughout the extratropics. While convection in midlatitudes is much less frequent than in the tropics, the relative humidity on the 380-K surface is much lower in midlatitudes and therefore the convective contrast is high, so the convective tendency reaches a maximum in this region.

[30] Thus our isentropic model simulations confirm that the effects of convection are different for different constituents. Convection at 10°N, for example, has an important effect on O_3 but a relatively small one on H_2O; convection at 50°N, conversely, has an important effect on H_2O but a negligible one on O_3. Because the convective contrast for O_3 is relatively constant, horizontal variations in the effects of convection on O_3 tend to be driven by horizontal variations in τ_c. For H_2O, on the other hand, horizontal variations in the effects of convection are driven by variations in both τ_c and convective contrast.

[31] That convection has little effect on O_3 in the midlatitudes at 380 K might seem surprising. After all, the HALOE O_3 plot in Figure 2 shows that there is a broad low-O_3 region associated with the Asian monsoon anticyclone, a region of vigorous convection. One might have reasonably assumed that these low VMRs were the result of convection. It turns out, however, that an O_3 minimum appears there in our model whether convection is turned on or not.

[32] The O_3 minimum appears over the monsoon region because once air gets into the monsoon region, it becomes "trapped" in the anticyclone (e.g., see the trajectory calculations plotted in Figure 5 of *Dethof et al.* [1999]). As the air repeatedly circulates around the anticyclone, even the slow Brewer-Dobson circulation can significantly lower the O_3 VMR. That is not the case over North America, where the weaker convection does not produce a closed circulation. That is not to say that convection has no effect here. O_3 VMRs in the Asian monsoon in our model with convection turned on are ~60% of the VMRs when convection is turned off.

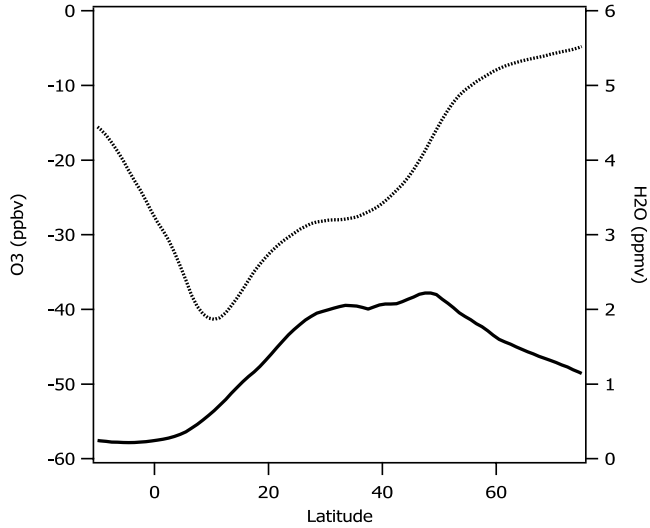

Figure 8. Differences between the zonal average H_2O (solid line, right-hand axis, in ppmv) and O_3 (dotted line, left-hand axis, in ppbv) predicted by models with and without convection. Positive values mean that the model with convection predicts higher VMRs for a constituent; negative values mean the opposite. The time period simulated is July 1993–1999.

[33] Because of this, three-dimensional chemistry-transport models can be expected to do a reasonable job of simulating O_3 on the 380-K surface, despite the well-documented limitations of their convective parameterizations [e.g., *Emanuel and Raymond*, 1993]. However, on the basis of our work here, we conclude that successfully simulating the O_3 fields at 380 K does not provide any confidence that the model's H_2O fields or convective processes are reasonable.

[34] We can also now explain the questions posed in the beginning of this paper. We noted in both the satellite and in situ data that air over North America presented a conundrum: high H_2O (>10 ppmv), consistent with upward transport, but high O_3 (>400 ppbv), not consistent with upward transport. Our work in this paper presents an explanation. Air at 380 K over North America is, by and large, stratospheric. Midlatitude convection transports little mass to these levels of the atmosphere. However, because of the large convective contrast for H_2O here, transport of even a small amount of mass can significantly moisten the stratosphere. Such convection, however, leaves the O_3 largely unchanged. Such a conclusion is qualitatively consistent with a tracer analysis of *Ray et al.* [2004], which showed that air at these altitudes over North America retained a predominantly stratospheric character, despite clearly being perturbed by convection.

[35] The CRYSTAL in situ data in Figure 1 show that the influence of convection (as represented by measurements with H_2O VMRs > 7 ppmv) drops off rapidly above 380 K, and is entirely gone by 400 K. The fact that the midlatitude convection penetrates to such high altitudes is significant. 390-K θ is $\sim$10–15 K above the tropical cold-point tropopause. Thus, if this convectively influenced air is transported isentropically to the upwelling equatorial region, it can be lofted into the main bulk of the overworld stratosphere without ever crossing the tropical cold point.

[36] Initial investigations using our model suggest that such transport is likely not important. Model runs where extratropical convection is turned off show little change in tropical H_2O VMRs. The reason is that the tropics are maintained near saturation by slow upwelling and convective transport. There is little room for increasing the H_2O there in our model unless supersaturation is allowed. In addition, most of the moistening from extratropical convection occurs on the warm, poleward flank of the extratropical convective regions. Being located well in the midlatitudes, significant amounts of this air appear not to make it into the tropics. This conclusion must be considered tentative, however, and more work must be done to verify it.

4. Relation to Tropical Dehydration

[37] We have argued in previous publications that convection in the tropics reaching the tropopause, i.e., into the TTL, may dehydrate the air there by detraining H_2O mixing ratios lower than those prevailing in the environment [*Sherwood and Dessler*, 2000, 2001]. That model successfully simulated the abundance of water [*Sherwood and Dessler*, 2001] and water's isotopologues [*Dessler and Sherwood*, 2003] in the TTL and stratosphere, and produced reasonable seasonal cycles of H_2O and a CO_2-like passive tracer in the tropical stratosphere [*Sherwood and Dessler*, 2003].

[38] The parameterization we present in equation (1), a relaxation to saturation, predicts a zero tendency from convection in regions where the atmosphere is saturated, and a negative tendency in regions where the atmosphere is supersaturated. Such saturated or supersaturated conditions often do occur in the tropics [e.g., *Jensen et al.*, 1999]. Under such conditions, details of ice microphysical processes that are relatively unimportant in regions of rapid evaporation might become important and lead to deviations from the simple behavior predicted by equation (1). Our work in this paper sheds no light on the issue of convective moisture tendencies in the tropics; clearly, more work on it is necessary to resolve the issues involved.

5. Conclusions

[39] By differencing the model runs with and without convection, we estimate that deep convection (primarily intense continental thunderstorms over Asia and North America) increases northern hemisphere extratropical H_2O (averaged over the region poleward of 30°N) on the 380-K potential temperature surface by about 40% during summer, while decreasing O_3 by $\sim$6%. While these numbers must be treated as rough estimates, we believe that the success of the model in reproducing zonal variations of both tracers leaves no doubt that local deep convection is an important component of the H_2O budget of the extratropical lower stratosphere during this time, but much less important for O_3. It also seems certain that the H_2O abundance of the entire altitude range of the summertime lowermost stratosphere, and even the bottom of the overworld, is influenced by deep convection.

[40] That convection can moisten even the overworld is potentially significant, in that the moisture can be transported isentropically to the tropics [*Minschwaner et al.*, 1996] and then be lofted into the stratosphere without having to pass through the tropical cold-point tropopause, which is located $\sim$375 K. Our runs do not suggest that this contributes significantly to water vapor in the upwelling regions. However, our model is not ideally suited to test this idea and this issue deserves further study.

[41] Our analysis suggests that convection plays a minor role in regulating extratropical O_3 at 380 K. Rather, the O_3 distribution is primarily determined by horizontal advection and the slow Brewer-Dobson circulation. This is true even of the O_3 minimum over the Asian monsoon, which arises not from convective transport but primarily from large-scale dynamics. This accounts for the lack of a corresponding O_3 minimum over North America, where the flow is predominantly zonal and there is little trapping of air in the region.

[42] We have argued that convection affects H_2O and O_3 differently owing to differences in what we term the "convective contrast": the difference between the abundance of a constituent in a convective outflow and in the ambient environment. At midlatitudes, where the relative humidity of the lower stratosphere is low (and therefore the saturation VMR $\gg$ [H_2O]), even infrequent convection can transport significant H_2O. Such convection, however, has only a small effect on the abundance of O_3. This provides an explanation for the puzzling observations of air with stratospheric O_3 (>400 ppbv) and tropospheric H_2O (>10 ppmv).

[43] The convective contrast is high for H_2O in the extratropics because of low relative humidities. To understand why this occurs, first notice from Figure 7 that the H_2O VMR is, within a factor of about two, constant on the 380-K surface. Air transported isentropically out of the tropics as well as that descending to the 380-K surface from higher altitudes have both been dehydrated to VMRs consistent with the temperatures at the tropical tropopause [e.g., *Dessler*, 1998]. At the same time, the 380-K isentrope descends in altitude as one proceeds poleward, warming substantially as it does so. This leads to saturation VMRs in the extratropics greatly in excess of the local H_2O VMRs. Thus it is ultimately the temperature difference between the tropics and extratropics at 380 K that determines the difference between the ambient H_2O VMR and the saturation VMR and therefore allows significant moistening by such small inputs of tropospheric air. If the 380-K isentrope had a constant temperature, then it would be nearly saturated everywhere and there would be no increase in convective contrast with latitude and likely no H_2O maxima associated with the monsoon circulations.

[44] In summary, this work suggests that, in the summer at least, deep convection plays an important part of the overall budget of H_2O at $\sim$380 K and below in the midlatitudes. As a result, trends in convective moistening might be playing a role in H_2O trends in the midlatitude lowermost stratosphere. Such trends could arise from either

trends in the amount of convective mass flux or trends in the convective contrast ($[H_2O]_c$-$[H_2O]$). Trends in convective contrast can arise because of changes in the latitude of convection, microphysical changes affecting the delivery of ice to the highest levels reached, or changes in the temperature difference between the tropics and extratropics. This latter might change as our climate changes, for example, because of changes in wave-driven stratospheric overturning. These possibilities should be considered in assessing trends in the instrumental record of lower stratospheric water vapor below ~390-K potential temperature.

[45] **Acknowledgments.** We acknowledge the army of scientists who produced the data used in this paper: J. M. Russell III et al. (HALOE H_2O and O_3), J. W. Waters and W. G. Read et al. (MLS H_2O), E. M. Weinstock et al. (WB-57 H_2O), E. Richard et al. (WB-57 O_3), T. T. Thompson et al. (WB-57 temperature and pressure), and W. B. Rossow et al. (ISCCP B3 radiances). Without their hard work, this analysis would not have been possible. Useful discussions with Dan Kirk-Davidoff, Eric Jensen, Paul Newman, Bill Read, and Ellis Remsberg are acknowledged. This work was supported by a NASA New Investigator Program grant to the University of Maryland, a NASA EOS/IDS grant to the University of Maryland and Yale University, and a NASA CRYSTAL-FACE grant to the University of Maryland and Yale University.

References

Alcala, C. M., and A. E. Dessler (2002), Observations of deep convection in the tropics using the TRMM precipitation radar, *J. Geophys. Res.*, *107*(D24), 4792, doi:10.1029/2002JD002457.

Barath, F. T., et al. (1993), The Upper Atmosphere Research Satellite Microwave Limb Sounder instrument, *J. Geophys. Res.*, *98*, 10,751–10,762.

Dessler, A. E. (1998), A reexamination of the "stratospheric fountain" hypothesis, *Geophys. Res. Lett.*, *25*, 4165–4168.

Dessler, A. E. (2002), The effect of deep, tropical convection on the tropical tropopause layer, *J. Geophys. Res.*, *107*(D3), 4033, doi:10.1029/2001JD000511.

Dessler, A. E., and H. Kim (1999), Determination of the amount of water vapor entering the stratosphere based on HALOE data, *J. Geophys. Res.*, *104*, 30,605–30,607.

Dessler, A. E., and S. C. Sherwood (2003), A model of HDO in the tropical tropopause layer, *Atmos. Chem. Phys.*, *3*, 2173–2181.

Dessler, A. E., M. D. Burrage, J.-U. Grooss, J. R. Holton, J. L. Lean, S. T. Massie, M. R. Schoeberl, A. R. Douglass, and C. H. Jackman (1998), Selected science highlights from the first five years of the Upper Atmosphere Research Satellite (UARS) program, *Rev. Geophys.*, *36*, 183–210.

Dethof, A., A. O'Neill, J. M. Slingo, and H. G. J. Smit (1999), A mechanism for moistening the lower stratosphere involving the Asian summer monsoon, *Q. J. R. Meteorol. Soc.*, *125*, 1079–1106.

Dunkerton, T. J. (1995), Evidence of meridional motion in the summer lower stratosphere adjacent to monsoon regions, *J. Geophys. Res.*, *100*, 16,675–16,688.

Ehhalt, D. H., and A. Tönnißen (1979), Hydrogen and carbon compounds in the stratosphere, in *Proceedings of the NATO Advanced Study Institute on Atmospheric Ozone: Its Variations and Human Influences*, edited by A. C. Aikin, pp. 129–151, U.S. Dep. of Transp., Washington, D. C.

Emanuel, K. A., and D. J. Raymond (1993), *The Representation of Cumulus Convection in Numerical Models*, 246 pp., Am. Meteorol. Soc., Boston, Mass.

Fischer, H., et al. (2003), Deep convective injection of boundary layer air into the lowermost stratosphere at midlatitudes, *Atmos. Chem. Phys.*, *3*, 739–745.

Fromm, M. D., and R. Servranckx (2003), Transport of forest fire smoke above the tropopause by supercell convection, *Geophys. Res. Lett.*, *30*(10), 1542, doi:10.1029/2002GL016820.

Fromm, M., J. Alfred, K. Hoppel, J. Hornstein, R. Bevilacqua, E. Shettle, R. Servranckx, Z. Q. Li, and B. Stocks (2000), Observations of boreal forest fire smoke in the stratosphere by POAM III, SAGE II, and lidar in 1998, *Geophys. Res. Lett.*, *27*, 1407–1410.

Gettelman, A., M. L. Salby, and F. Sassi (2002), Distribution and influence of convection in the tropical tropopause region, *J. Geophys. Res.*, *107*(D10), 4080, doi:10.1029/2001JD001048.

Holton, J. R., P. H. Haynes, M. E. McIntyre, A. R. Douglass, R. B. Rood, and L. Pfister (1995), Stratosphere-troposphere exchange, *Rev. Geophys.*, *33*, 403–439.

Hoskins, B. J. (1991), Towards a PV-θ view of the general circulation, *Tellus, Ser. A*, *43*(4), 27–35.

Jensen, E. J., W. G. Read, J. Merganthaler, B. J. Sandor, L. Pfister, and A. Tabazadeh (1999), High humidities and subvisible cirrus near the tropical tropopause, *Geophys. Res. Lett.*, *26*, 2347–2350.

Jost, H.-J., et al. (2004), In-situ observations of mid-latitude forest fire plumes deep in the stratosphere, *Geophys. Res. Lett.*, *31*, L11101, doi:10.1029/2003GL019253.

Livesey, N. J., M. D. Fromm, J. W. Waters, G. L. Manney, M. L. Santee, and W. G. Read (2004), Enhancements in lower stratospheric CH_3CN observed by the Upper Atmosphere Research Satellite Microwave Limb Sounder following boreal forest fires, *J. Geophys. Res.*, *109*, D06308, doi:10.1029/2003JD004055.

Minschwaner, K., A. E. Dessler, J. W. Elkins, C. M. Volk, D. W. Fahey, M. Loewenstein, J. R. Podolske, A. E. Roche, and K. R. Chan (1996), Bulk properties of isentropic mixing into the tropics in the lower stratosphere, *J. Geophys. Res.*, *101*, 9433–9439.

Poulida, O., R. R. Dickerson, and A. Heymsfield (1996), Stratosphere-troposphere exchange in a midlatitude mesoscale convective complex: 1. Observations, *J. Geophys. Res.*, *101*, 6823–6836.

Proffitt, M. H., and R. J. McLaughlin (1983), Fast-response dual-beam UV-absorption ozone photometer suitable for use on stratospheric balloons, *Rev. Sci. Instrum.*, *54*, 1719–1728.

Randel, W. J., F. Wu, and D. J. Gaffen (2000), Interannual variability of the tropical tropopause derived from radiosonde data and NCEP reanalysis, *J. Geophys. Res.*, *105*, 15,509–15,523.

Randel, W. J., F. Wu, A. Gettelman, J. M. Russell III, J. M. Zawodny, and S. J. Oltmans (2001), Seasonal variation of water vapor in the lower stratosphere observed in Halogen Occultation Experiment data, *J. Geophys. Res.*, *106*, 14,313–14,325.

Ray, E. A., et al. (2004), Evidence of the effect of summertime midlatitude convection on the subtropical lower stratosphere from CRYSTAL-FACE tracer measurements, *J. Geophys. Res.*, *109*, D18304, doi:10.1029/2004JD004655.

Read, W. G., D. L. Wu, J. W. Waters, and H. C. Pumphrey (2004), A new 147–56 hPa water vapor product from the UARS Microwave Limb Sounder, *J. Geophys. Res.*, *109*, D06111, doi:10.1029/2003JD004366.

Roach, W. T. (1967), On nature of summit areas of severe storms in Oklahoma, *Q. J. R. Meteorol. Soc.*, *397*, 318–336.

Rosenfield, J. E., P. A. Newman, and M. R. Schoeberl (1994), Computations of diabatic descent in the stratospheric polar vortex, *J. Geophys. Res.*, *99*, 16,677–16,689.

Russell, J. M., III, et al. (1993), The Halogen Occultation Experiment, *J. Geophys. Res.*, *98*, 10,777–10,797.

Sherwood, S. C., and A. E. Dessler (2000), On the control of stratospheric humidity, *Geophys. Res. Lett.*, *27*, 2513–2516.

Sherwood, S. C., and A. E. Dessler (2001), A model for transport across the tropical tropopause, *J. Atmos. Sci.*, *58*, 765–779.

Sherwood, S. C., and A. E. Dessler (2003), Convective mixing near the tropical tropopause: Insights from seasonal variations, *J. Atmos. Sci.*, *60*, 2674–2685.

Stainforth, A., and J. Cote (1991), Semi-Lagrangian integration schemes for atmospheric models: A review, *Mon. Weather Rev.*, *119*, 2206–2223.

Stratospheric Processes and their Role in Climate (SPARC) (2000), SPARC assessment of upper tropospheric and stratospheric water vapour, World Clim. Res. Program, Geneva.

Swinbank, R., and A. O'Neill (1994), A stratosphere-troposphere data assimilation system, *Mon. Weather Rev.*, *122*, 686–702.

Wang, P. K. (2003), Moisture plumes above thunderstorm anvils and their contributions to cross-tropopause transport of water vapor in midlatitudes, *J. Geophys. Res.*, *108*(D6), 4194, doi:10.1029/2002JD002581.

Weinstock, E. M., E. J. Hintsa, A. E. Dessler, J. F. Oliver, N. L. Hazen, J. N. Demusz, N. T. Allen, L. B. Lapson, and J. G. Anderson (1994), New fast response photofragment fluorescence hygrometer for use on the NASA ER-2 and the Perseus remotely piloted aircraft, *Rev. Sci. Instrum.*, *65*, 3544–3554.

Wofsy, S. C., J. C. McConnell, and M. B. McElroy (1972), Atmospheric CH_4, CO, and CO_2, *J. Geophys. Res.*, *77*, 4477–4493.

A. E. Dessler, ESSIC, University of Maryland, College Park, 2207 Computer and Space Science Building, College Park, MD 20742, USA. (dessler@atmos.umd.edu)

S. C. Sherwood, Department of Geology and Geophysics, Yale University, P. O. Box 208109, New Haven, CT 06520-8109, USA.